

Structural Dynamic Analysis of a Non Symmetrical RC Building within the Context of a Blind Prediction Contest

Adele Klein^a, Jan Moore^a, Yves Mondet^a, and Urs Bumann^b

^aBasler & Hofmann Consulting Engineers, CH-8032 Zurich, Switzerland, e-mail: Adele.Klein@bhz.ch

^bSwiss Federal Nuclear Safety Inspectorate, CH-5232 Villigen-ENSI, Switzerland

Keywords: Reinforced concrete, Non-symmetric, Non-linear, Dynamic time-history, Shaking table.

1 ABSTRACT

The Commissariat à l'Énergie Atomique (CEA) launched a blind prediction contest project entitled SMART 2008. The objective of this benchmark is to predict the dynamic behavior of a non-symmetric, 3-dimensional, reinforced concrete (RC) building designed in accordance with French nuclear design methods and subjected to seismic excitation. The experimental tests have been carried out with a well instrumented, three-dimensional, RC specimen on the AZALEE shaking table at CEA. The team of ENSI (Swiss Federal Nuclear Safety Inspectorate) and Basler & Hofmann Consulting Engineers has developed several linear and non-linear analytical models to best predict the results from these experimental tests. Development of these models and comparisons of their predictions are presented in this paper. A modeling study has been conducted with three parts: 1) a comparison of non-linear, linear best estimate, and linear design practice models, 2) a refined non-linear investigation regarding the importance of considering non-linearities from previous test runs, and 3) a refined non-linear investigation highlighting the importance of considering out-of-plane stiffness degradation from concrete cracking.

2 INTRODUCTION

The SMART 2008 project was launched in May, 2007 and will conclude with a final workshop in 2010. More than 30 international teams consisting of industry, nuclear/energy corporations, and research facilities are taking part in this blind prediction contest. The project consists of two phases: Phase 1 - seismic analysis of a nuclear reinforced concrete building, and Phase 2 - variability quantification and fragility assessment. This paper focuses on Phase 1 work conducted between May, 2007 and December, 2008 by the team of ENSI (Swiss Federal Nuclear Safety Inspectorate) and Basler & Hofmann Consulting Engineers. The SMART 2008 organizers, CEA/EDF, developed a shaking table experiment in order to investigate the behavior of a non-symmetric, concrete specimen under seismic loading. The objective of this work was to develop a model that best predicts the seismic response of the SMART 2008 test specimen. Due to contractual agreements with CEA, we are unable to present structural response data from the experiment (except recorded ground motion input) at the time of publication. Therefore, this paper describes only our modeling outcomes.

3 DESCRIPTION OF THE "SMART 2008" TEST SETUP

The specimen was tested in 2008 on the AZALEE shaking table at Commissariat à l'Énergie Atomique (CEA Saclay, France). **Figure 1**, provided by CEA, shows the general test setup. Continuous reinforced concrete footings were provided at the base of the walls and at the base of the columns. In order to provide a solid attachment to the shaking table, embedded concrete reinforcement was welded to a 2 cm thick steel base plate. The base plate is then directly bolted to the shaking table. The shaking table can be idealized as a 25 t rigid block with four horizontal and four vertical hydraulic jacks. The jacks are active systems, meaning they are operated by a control system during the experiment.

To understand the performance of the structure under different levels of excitation, the specimen was subjected sequentially to 13 biaxial, horizontal, synthetic-input ground motions, each with increased

intensity. The time of the accelerograms has been scaled by a factor of two to correspond to the quarter scale of the model. **Figure 2a** shows the progression of shaking table simulated ground motion in terms of peak ground accelerations (PGA), which were recorded from the table during each test.



Figure 1. Photo of SMART 2008 structure and shaking table test setup (CEA).

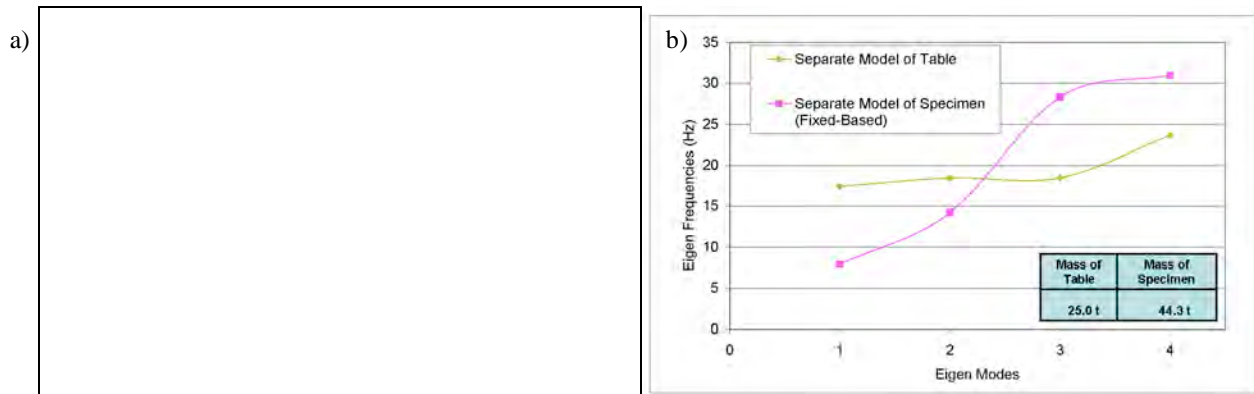


Figure 2. a) PGA of simulated ground motions for each test run (Lermitte and Chaudat, 2008). b) Modal comparison of table and fixed-based specimen considered separately.

The specimen was fully instrumented. Accelerometers were mounted on the slabs, walls, and footings of the specimen. Strain gages were placed on the vertical reinforcing bars where non-linear behavior was expected. For this specimen, non-linear behavior was anticipated at the base and edges of the U-shaped concrete shear wall. The shaking table itself is instrumented with X and Y direction accelerometers mounted to the center of the table's upper face, and vertical accelerometers (Z direction) mounted to the four corners of the table (Lermitte and Chaudat, 2008).

4 CONSIDERATIONS FOR MODELING THE "SMART 2008" TEST SETUP

4.1 Influence and Modeling of the Shaking Table

The shaking table control system was designed to limit the shaking table motion to only the X and Y principle horizontal directions. However, significant rigid body motion (i.e. pitch, roll, and yaw) of the table was also observed during the tests. In order to accurately model the test results, this undesired table motion was also included. Using the finite element program SAP 2000, a modal analysis was conducted of the shaking table and the specimen (with a fixed-base) separately. From this modal analysis, **Figure 2b** shows a comparison of the calculated frequencies of the first four Eigen modes as well as a comparison of the masses. Due to the coupled nature of the table and the specimen, the specimen and the underlying table had to be considered as one system.

The shaking table was idealized as a nodal mass with 25 t translational mass, 80 tm^2 rotational mass around the x and y axis (pitch and roll), and 180 tm^2 rotational mass around the z axis (yaw). The 8 active jacks were modeled as parallel springs and dampers. The spring and damper elements, the table mass node, and the base nodes of the building model were interconnected with rigid beam elements.

The spring stiffness's were varied until the modal frequencies and the acceleration and displacement response spectra of the model best matched the associated shaking table test results from run 4. The run 4 response was chosen to calibrate the model because while the ground motion was significantly large, the model remains relatively elastic during the shaking table test. The spring stiffness's used were 75 MN/m for the vertical springs and 80 MN/m for the horizontal springs. These values were held constant for all models and all time history runs. The damping values were set specific to each time history run to account for the fact that energy dissipation of the active control system will vary depending of the ground motion input. The damping constant, c (KNs/m), was varied until the acceleration and displacement response spectrums of the model best matched the associated shaking table test results for each run.

4.2 Modeling the Concrete Building Specimen

At the end of our modeling campaign, three distinct dynamic time history models were developed, each representing a level of refinement. The model assumptions are summarized for the three modeling cases in **Table 1**. The least refined model is a linear finite element model developed with SAP2000. This model contains assumptions commonly used in conventional Swiss Nuclear Power Plant design practice. It assumes a constant elastic modulus, in this case 32 GPa, and nonlinearity is accounted for using a high Rayleigh damping ratio of 7% common for SSE calculations. The most refined model, on the other hand, is the non-linear analysis developed using the fiber element program, PERFORM 3D. The experimental data indicates that the initial damping value of the first three modes is between 1 and 2% (Lermitte and Chaudat, 2008). Accordingly, the assigned damping is set low at 1% Rayleigh damping for this model. The intermediate model is a linear finite element model considered the best-estimate using conventional design software, in this case SAP 2000. As in the most refined model, the assigned damping ratio is set to 1% Rayleigh damping. For each time history run, the elastic modulus was modified to account for the effective cracked stiffness. For each time history run, the elastic modulus was varied until the modal frequencies of the model best-fit the specimen's modal frequencies. **Figure 3** shows a comparison of the modal frequencies from the various models. It also shows the effective cracked stiffness used in the Linear Analysis Best Estimate model in order to best match the experimental data.

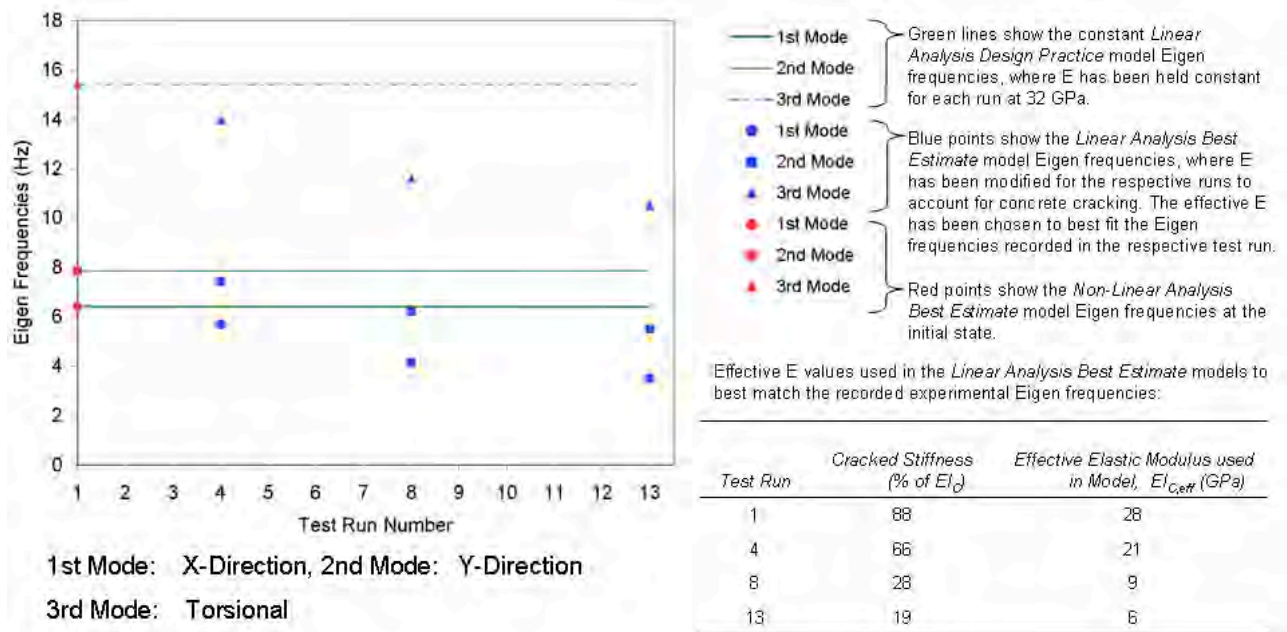


Figure 3. Comparison of model Eigen frequencies through the test sequence.

Table 1. Comparison of basic model assumptions

	Elements/ Variables	Linear Analysis Design Practice	Linear Analysis Best Estimate	Non-Linear Analysis Best Estimate																		
SPECIMEN	Walls	Linear elastic isotropic shell elements		Nonlinear fiber shell elements with: <ul style="list-style-type: none"> • Nonlinear fibers for in plane loading • Linear elements for out of plane loading: (2 variations considered) <ul style="list-style-type: none"> - E= 28 GPa for all runs - E varied for all runs: <table border="0"> <tr> <td>$E_{RUN1} = 28 \text{ GPa}$</td> <td>$E_{RUN8} = 9 \text{ GPa}$</td> </tr> <tr> <td>$E_{RUN4} = 21 \text{ GPa}$</td> <td>$E_{RUN13} = 6 \text{ GPa}$</td> </tr> </table> 	$E_{RUN1} = 28 \text{ GPa}$	$E_{RUN8} = 9 \text{ GPa}$	$E_{RUN4} = 21 \text{ GPa}$	$E_{RUN13} = 6 \text{ GPa}$														
	$E_{RUN1} = 28 \text{ GPa}$	$E_{RUN8} = 9 \text{ GPa}$																				
	$E_{RUN4} = 21 \text{ GPa}$	$E_{RUN13} = 6 \text{ GPa}$																				
	Wall base	Linear elastic isotropic shell elements		Nonlinear fiber shell elements with: <ul style="list-style-type: none"> • Nonlinear fibers for vertical loading • Linear elements for loading in all other directions 																		
	Slabs	Linear isotropic shell elements		Linear isotropic shell elements, $\nu = 0.2$																		
Beams	Linear elastic beam elements		Linear isotropic shell elements. Not modeled separately, included in the slabs.																			
Columns	Linear elastic beam elements		Nonlinear fiber beam elements																			
TABLE	Nodal mass	Nodal mass located at X/Y/Z = 1.5/0.94/-0.77 with masses $m_x = m_y = m_z = 25 \text{ t}$. The node is assigned $m_{pitch} = m_{roll} = 80 \text{ tm}^2$, $m_{yaw} = 180 \text{ tm}^2$ moments of inertia. The nodal mass is connected to the specimen's support node (at X/Y/Z = 1.28/0.92/-0.0) and the jacks by rigid beams.																				
	Rigid beams	Beam elements with an assigned $E = 1'000 \text{ GPa}$ and a cross section of 10x10 m.																				
JACKS	Vertical dampened springs	Each modeled as a parallel spring and damper with $k = 75 \text{ MN/m}$ and $c_{RUN1} = 300 \text{ KNs/m}$, $c_{RUN4} = 150 \text{ KNs/m}$, $c_{RUN8} = 750 \text{ KNs/m}$, $c_{RUN13} = 850 \text{ KNs/m}$																				
	Horizontal dampened springs	Each modeled as a parallel spring and damper with $k = 80 \text{ MN/m}$ and $c = 0 \text{ KNs/m}$																				
INTER-FACE	Boundary conditions	Support node (at X/Y/Z = 1.28/0.92/0.0) is fixed in the X and Y DOF. Z DOF of vertical jacks is fixed. X and Y DOF of horizontal jacks is fixed.																				
	Acceleration input	Recorded acceleration time histories are applied to the nodes fixed in the x and y directions.																				
MATERIAL	Material constitutive law for concrete in compression/ tension	C30/37 Concrete type. assumed to remain linearly elastic, reinforced concrete modeled as one material:	<ul style="list-style-type: none"> • Run 1: $E = 28 \text{ GPa}$, $G = 11.7 \text{ GPa}$ • Run 4: $E = 21 \text{ GPa}$, $G = 8.75 \text{ GPa}$ • Run 8: $E = 9.0 \text{ GPa}$, $G = 3.75 \text{ GPa}$ • Run 13: $E = 6.0 \text{ GPa}$, $G = 2.5 \text{ GPa}$ 	<p>Strain hardening, strength degradation modeled:</p> <table border="1"> <thead> <tr> <th>Point</th> <th>Stress (MPa)</th> <th>Strain</th> </tr> </thead> <tbody> <tr><td>T1</td><td>4.00E+07</td><td>1.00E-07</td></tr> <tr><td>T2</td><td>3.50E+04</td><td>3.00E+01</td></tr> <tr><td>T3</td><td>2.50E+04</td><td>3.00E+01</td></tr> <tr><td>T4</td><td>2.50E+04</td><td>3.00E+01</td></tr> <tr><td>T5</td><td>3.00E+01</td><td>3.00E+01</td></tr> </tbody> </table>	Point	Stress (MPa)	Strain	T1	4.00E+07	1.00E-07	T2	3.50E+04	3.00E+01	T3	2.50E+04	3.00E+01	T4	2.50E+04	3.00E+01	T5	3.00E+01	3.00E+01
	Point	Stress (MPa)	Strain																			
	T1	4.00E+07	1.00E-07																			
T2	3.50E+04	3.00E+01																				
T3	2.50E+04	3.00E+01																				
T4	2.50E+04	3.00E+01																				
T5	3.00E+01	3.00E+01																				
Material constitutive law for concrete in shear	C30/37 Concrete type. assumed to remain linearly elastic, reinforced concrete modeled as one material:	<ul style="list-style-type: none"> • Run 1: $E = 28 \text{ GPa}$, $G = 11.7 \text{ GPa}$ • Run 4: $E = 21 \text{ GPa}$, $G = 8.75 \text{ GPa}$ • Run 8: $E = 9.0 \text{ GPa}$, $G = 3.75 \text{ GPa}$ • Run 13: $E = 6.0 \text{ GPa}$, $G = 2.5 \text{ GPa}$ 	<p>Modeled as elastic perfectly plastic:</p> <table border="1"> <thead> <tr> <th>Point</th> <th>Stress (MPa)</th> <th>Strain</th> </tr> </thead> <tbody> <tr><td>T1</td><td>1.00E+02</td><td>1.00E-02</td></tr> <tr><td>T2</td><td>1.00E+02</td><td>1.00E-02</td></tr> <tr><td>C1</td><td>-1.00E+02</td><td>-1.00E-02</td></tr> <tr><td>C2</td><td>-1.00E+02</td><td>-1.00E-02</td></tr> <tr><td>C3</td><td>-1.00E+04</td><td>-1.00E-02</td></tr> </tbody> </table>	Point	Stress (MPa)	Strain	T1	1.00E+02	1.00E-02	T2	1.00E+02	1.00E-02	C1	-1.00E+02	-1.00E-02	C2	-1.00E+02	-1.00E-02	C3	-1.00E+04	-1.00E-02	
Point	Stress (MPa)	Strain																				
T1	1.00E+02	1.00E-02																				
T2	1.00E+02	1.00E-02																				
C1	-1.00E+02	-1.00E-02																				
C2	-1.00E+02	-1.00E-02																				
C3	-1.00E+04	-1.00E-02																				
Material law for steel in compression/ tension	Steel reinforcement was not modeled separately.		<p>Modeled bi-linearly:</p> <table border="1"> <thead> <tr> <th>Point</th> <th>Stress (MPa)</th> <th>Strain</th> </tr> </thead> <tbody> <tr><td>T1</td><td>0.00E+00</td><td>1.00E-02</td></tr> <tr><td>T2</td><td>0.00E+00</td><td>6.00E+01</td></tr> <tr><td>C1</td><td>0.00E+00</td><td>-1.00E-02</td></tr> <tr><td>C2</td><td>0.00E+00</td><td>-7.00E+01</td></tr> </tbody> </table>	Point	Stress (MPa)	Strain	T1	0.00E+00	1.00E-02	T2	0.00E+00	6.00E+01	C1	0.00E+00	-1.00E-02	C2	0.00E+00	-7.00E+01				
Point	Stress (MPa)	Strain																				
T1	0.00E+00	1.00E-02																				
T2	0.00E+00	6.00E+01																				
C1	0.00E+00	-1.00E-02																				
C2	0.00E+00	-7.00E+01																				
Damping	7% Rayleigh damping	1% Rayleigh damping	1% Rayleigh damping																			
ANA-LYSIS	Analysis procedure	Linear time history analysis		Nonlinear time history analysis																		
	Analysis software	SAP2000 v11.0.6		PERFORM 3D v4.0.3																		

5 COMPARISON OF MODEL RESULTS

Although we are unable to make a direct comparison with experimental test data, the following section presents notable model comparison results. Our modeling study can be considered as three parts: 1) a comparison study of non-linear (with $E = 28$ GPa for out of plane loading), linear best estimate, and linear design practice models, 2) a refined non-linear study investigating the importance of considering non-linearities from previous test runs, and 3) a refined non-linear study investigating the importance of considering out-of-plane stiffness degradation from concrete cracking. Although the specimen has been subjected sequentially to 13 shaking table tests, the models were developed to consider only runs 1, 4, 8, and 13 as single events (starting from an uncracked condition for the non-linear models).

5.1 Comparison of Non-Linear, Linear Best Estimate, and Linear Design Practice Models

Figure 4 presents the peak horizontal acceleration responses for runs 1, 4, 8, and 13. The Linear Design Practice model, generally used in Swiss NPP design and evaluation for its conservative predictions, is shown to be the least conservative in predicting horizontal accelerations for the majority of the test runs. The concrete elastic modulus is held constant for the Linear Design Practice model at 32 GPa for each test, while the elastic modulus of the Linear Best Estimate model is varied between 88% (run 1) and 19% (run 13) of 32 GPa to simulate stiffness degradation from concrete cracking. In a fixed-base model, one would expect the stiffer structure to yield higher peak acceleration values. However, due to the coupled nature of the concrete specimen and the underlying shaking table, this stiffness-acceleration correlation does not hold in this case. This is also seen in **Figure 6**, which shows the 3rd floor horizontal acceleration FRS envelopes. **Figure 6** also shows how the Non-Linear Best Estimate model undergoes significant non-linear behavior in run 13, as the first Eigen frequency falls below the Linear Design Practice model's first Eigen frequency.

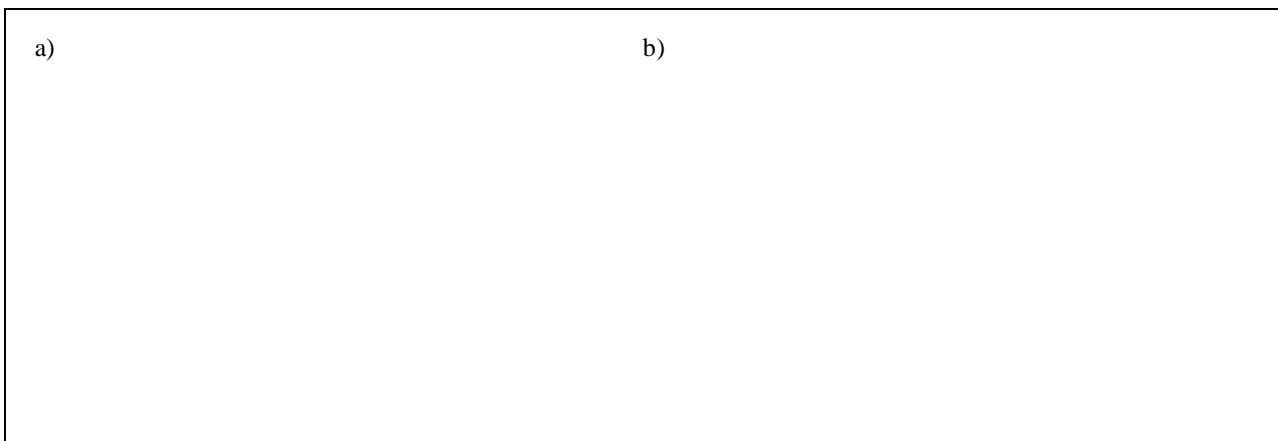


Figure 4. a) 3rd floor peak X-direction horizontal accelerations for runs 1, 4, 8, and 13. b) 3rd floor peak Y-direction horizontal accelerations for runs 1, 4, 8, and 13. (model results)

Figure 5 presents the peak horizontal displacement responses for runs 1, 4, 8, and 13. As expected, the Linear Design Practice model predicts the lowest peak displacements among the three different models due to its assumption of stiff uncracked concrete.

Nodal acceleration, displacement, and strain response time histories were calculated for later comparison with experimental test data. Strains were measured and calculated at locations where the concrete deformation was expected to be greatest. For the SMART 2008 specimen, the largest deformations were anticipated at the base of the shear walls, in the outer boundaries of the transverse walls. **Figure 7a** illustrates the location of the installed strain gages in the SMART 2008 specimen and the corresponding nodal locations in the analytical models.

Figure 7b and c show the calculated model peak strain values from runs 4 and 13, respectively. These figures demonstrate that strain in the boundary element of the shorter wall (J1V04, J2V04 and J6V04) is greater than the strain of the longer wall (J1V03, J2V03, and J9V03). There is also slightly greater strain at the base of the wall (110 mm above the top of the footing) than higher along the wall (675 mm above the top of the footing). As anticipated, the stiffest model, the Linear Design Practice model, yielded the smallest strain predictions. The Non-Linear Best Estimate model predicts the largest strain due to the fiber element modeling, which does not account for the tension resistance of the concrete between the cracks. If a fiber element reaches the tension strain of concrete, the stiffness and strength will be reduced to only the reinforcement.

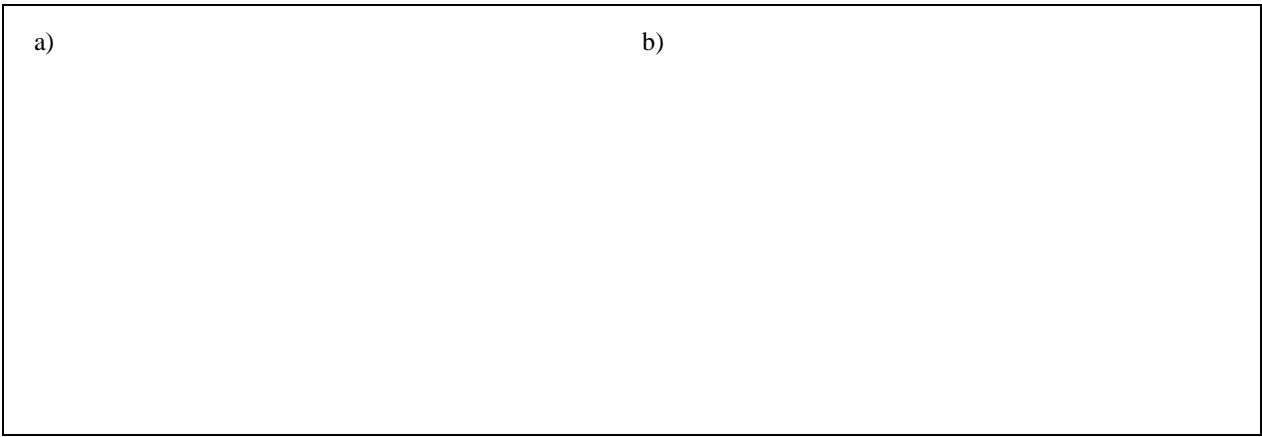


Figure 5. a) 3rd floor peak X-direction horizontal displacements for runs 1, 4, 8 and 13. b) 3rd floor peak Y-direction horizontal displacements for runs 1, 4, 8, and 13. (model results)

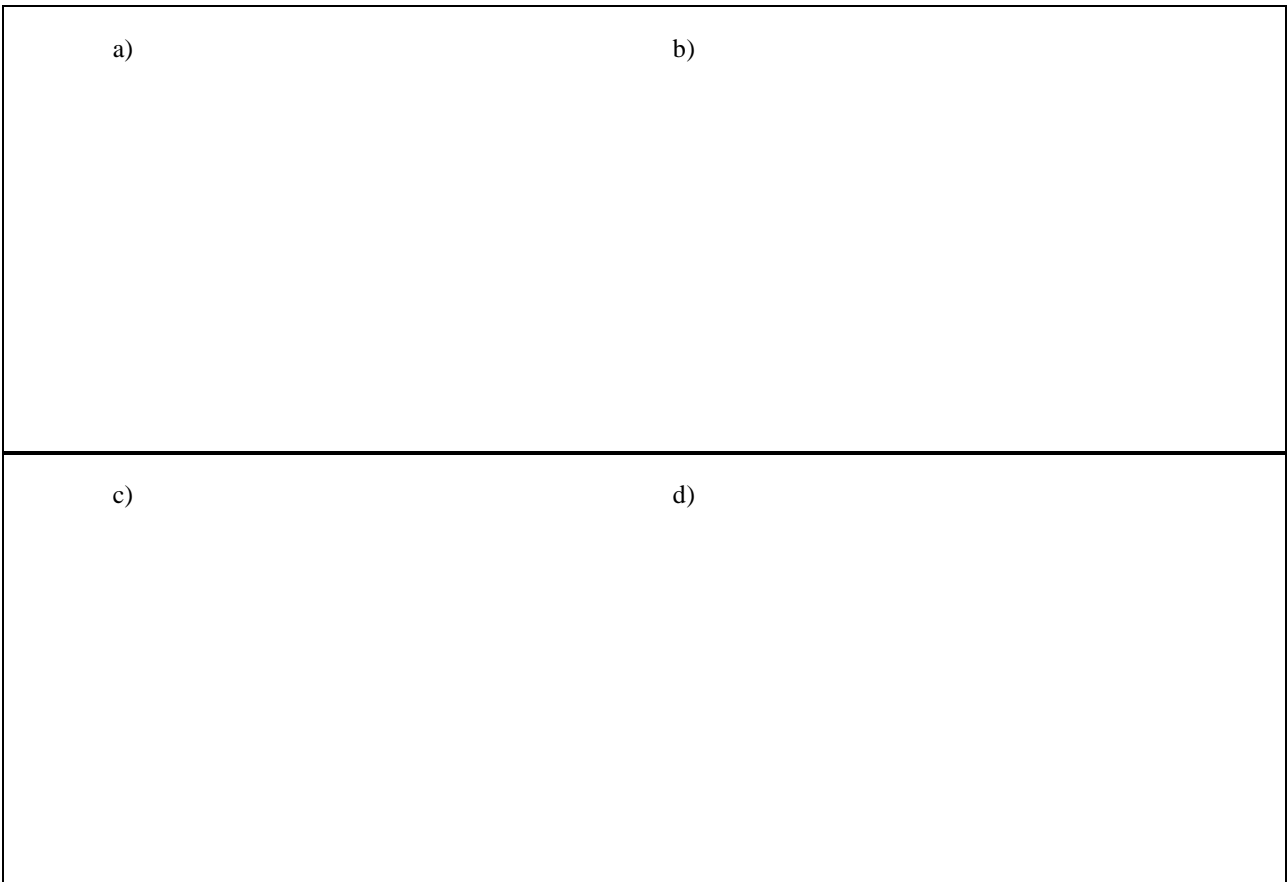


Figure 6. a) 3rd floor X-direction horizontal acceleration FRS envelopes for run 4. b) 3rd floor Y-direction horizontal acceleration FRS envelopes for run 4. c) 3rd floor X-direction horizontal acceleration FRS envelopes for run 13. d) 3rd floor Y-direction horizontal acceleration FRS envelopes for run 13. (model results)

Figure 8a-d show the strong motion strain time histories from run 4. Run 4 is the first in the testing sequence to have large enough ground motion to induce non-linear behavior in the Non-Linear Best Estimate model. **Figure 8b** shows that while the other recorded locations remain elastic, strain at the base of the short wall (J1,2V04) has exceeded an axial tension strain of 259 $\mu\epsilon$. Reviewing the assigned non-linear constitutive laws in **Table 1**, the modeled steel reinforcement remains elastic while the concrete exceeds its tension capacity at this location and retains no stiffness or strength (cracking has occurred). **Figure 9a-d** show strong motion strain time histories for run 13. Run 13 is the last in the testing sequence and has the largest input ground motion. **Figure 9b** shows that the upper portion of the long wall (J9V03) remains elastic and uncracked, while the base of the long wall (J1,2V03) and the base (J1,2V04) and the upper portion (J6V04) of the short wall show cracking over 259 $\mu\epsilon$ in the Non-Linear Best Estimate model. Additionally,

the calculated strain at the base of the short wall (J1,2V04) indicates permanent deformation, which occurs due to yielding of the reinforcement (strain over $2000 \mu\epsilon$, see **Table 1**). The Non-Linear Best Estimate model shows significant axial tension strains, which are due to the fact that after the concrete reaches an axial tension strain of over $259 \mu\epsilon$, the concrete loses its stiffness and strength. The axial tension is then taken only by the reinforcement, which results in low stiffness and therefore in large strains. Strain values predicted by the Non-Linear model at the base (J12 V03 and J1,2V04) may be high due to the fact that our model does not consider the reinforcement splice at the base of the walls. Additionally our fiber elements considered reinforcement and concrete behavior separately. Thus our model does not account for the improved axial properties of a well detailed and confined boundary element.

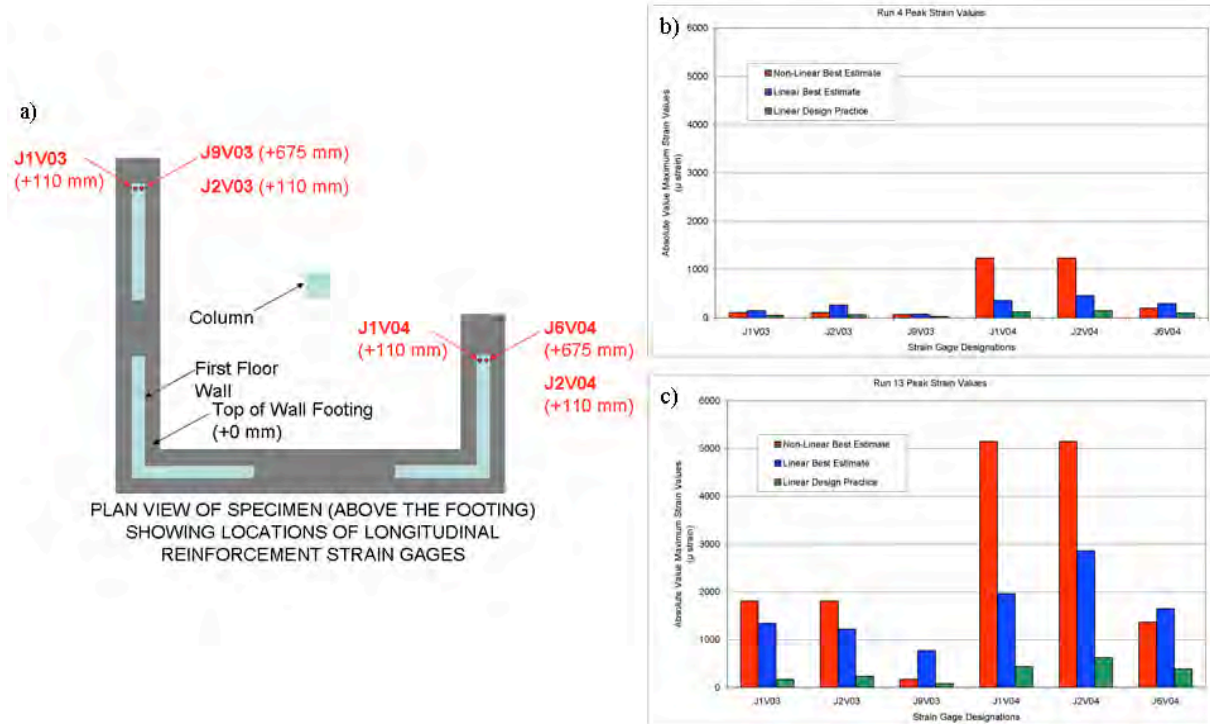


Figure 7. a) Diagram showing recorded/calculated strain locations (Information from Lermite & Chaudat, 2008). b) Model peak strain values for run 4. c) Model peak strain values for run 13.

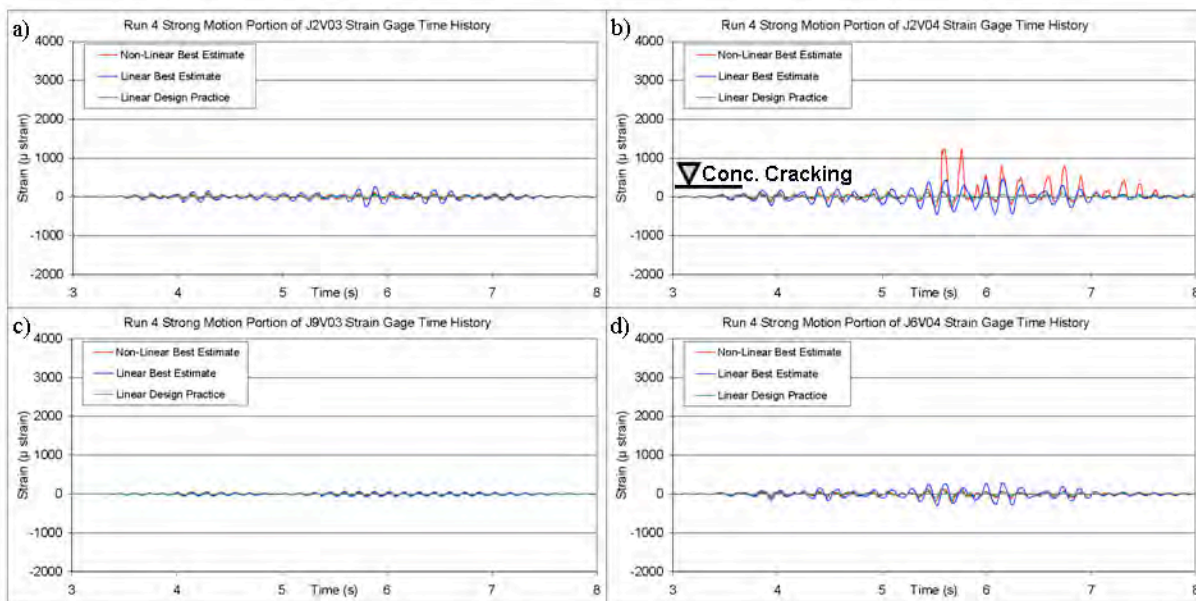


Figure 8. a) Strong motion portion of J2V03 strain gage time histories for run 4. b) Strong motion portion of J2V04 strain gage time histories for run 4. c) Strong motion portion of J9V03 strain gage time histories for run 4. d) Strong motion portion of J6V04 strain gage time histories for run 4. (model results)

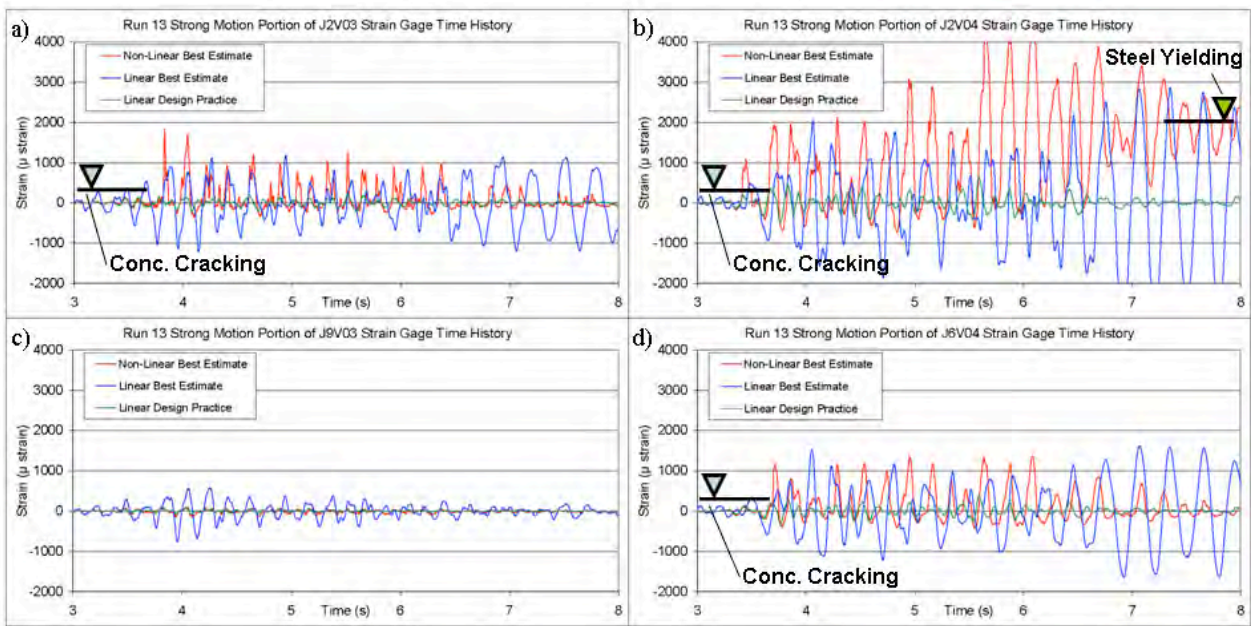


Figure 9. a) Strong motion portion of J2V03 strain gage time histories for run 13. b) Strong motion portion of J2V04 strain gage time histories for run 13. c) Strong motion portion of J9V03 strain gage time histories for run 13. d) Strong motion portion of J6V04 strain gage time histories for run 13. (model results)

5.2 Importance of Considering Non-Linearities from Previous Test Runs

Although the actual experiment was a sequence of tests, the model runs 1, 4, 8, and 13 were considered as single events. In the case of the Non-Linear model, the previous non-linearities were ignored and the starting condition was taken to be uncracked. This section investigates the validity of this assumption.

Figure 10 compares the strong motion acceleration and displacement response, for corner point C on the third floor in the Y-direction, between a non-linear model that considers only run 4 and one that considers also previous run sequences. This comparison shows that the time histories, as well as the FRS, are well correlated. Good correlation is expected since significant non-linear behavior is not expected in runs 1-3, and therefore it is reasonable to assume an uncracked state at the beginning of run 4.

Figure 11 and **Figure 12** compare the acceleration and displacement response between a non-linear model that considers only run 13 and the non-linear model that considers run sequence 10-13. The highlighted sections of the acceleration and displacement time histories show that the correlation is not as good as for run 4 at the beginning of the strong motion time history. As expected, the run sequence model shows a smaller initial frequency due to the already cracked initial state. Therefore it also shows higher displacement. The FRS comparison shows that the model only considering run 13 underestimates the important first frequency response by about 20%. Thus, in the case of SMART 2008 testing, the consideration of the run sequence seems to be appropriate. For even bigger inputs than run 13 with more inelastic deformation of the reinforcement it would be even more important.

5.3 Importance of Considering Realistic Out of Plane Stiffness Degradation

The Non-Linear models presented thus far have assumed linear elements for out of plane loading with an elastic modulus of 28 GPa, which is 88% of the uncracked concrete stiffness modulus. This section investigates the validity of this assumption and its appropriateness for run 13, the largest ground motion input run where more out of plane wall cracking may occur. **Figure 13** shows a comparison of acceleration FRS envelopes for the 3rd floor horizontal corner responses. The figure compares a non-linear model that considers run sequence 10-13 with an out of plane elastic modulus of 28 GPa and a non-linear model that considers run sequence 10-13 with an out of plane elastic modulus of 6 GPa (19% of the uncracked concrete stiffness). The results show that the modeled specimen response is relatively insensitive to out of plane elastic modulus variation. The structural behavior is governed by in plane motion and so reducing the out of plane elastic modulus by over 78% does not produce a significant change in response for this specimen.

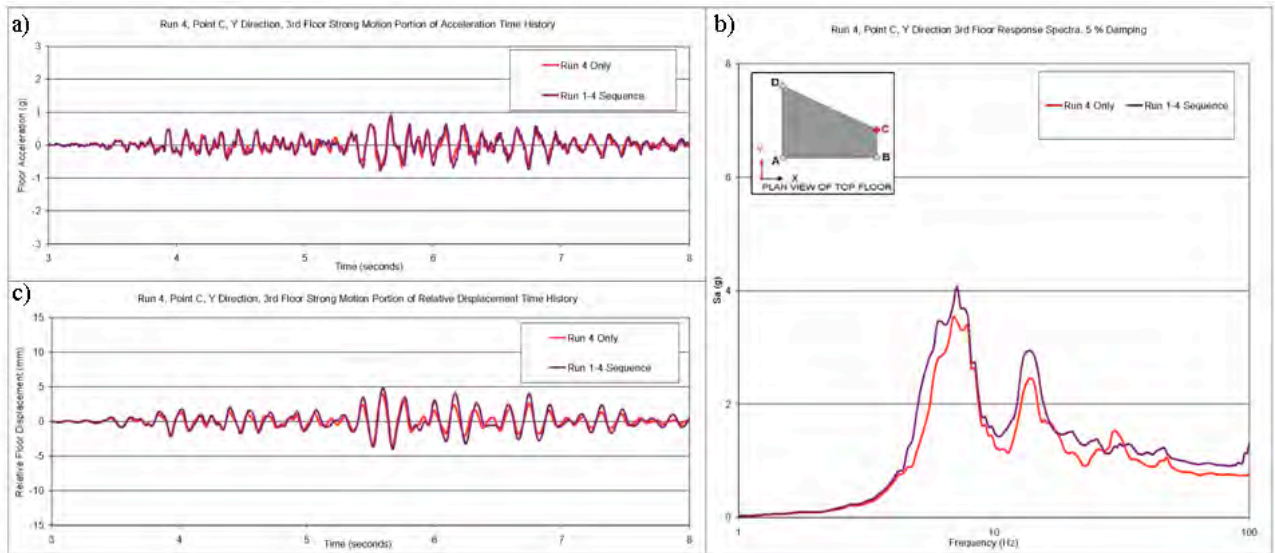


Figure 10. a) Strong motion portion of point C, Y-direction acceleration time histories for run 4. b) Acceleration FRS of point C, Y-direction for run 4. c) Strong motion portion of point C, Y-direction displacement time histories for run 4. (non-linear model results)

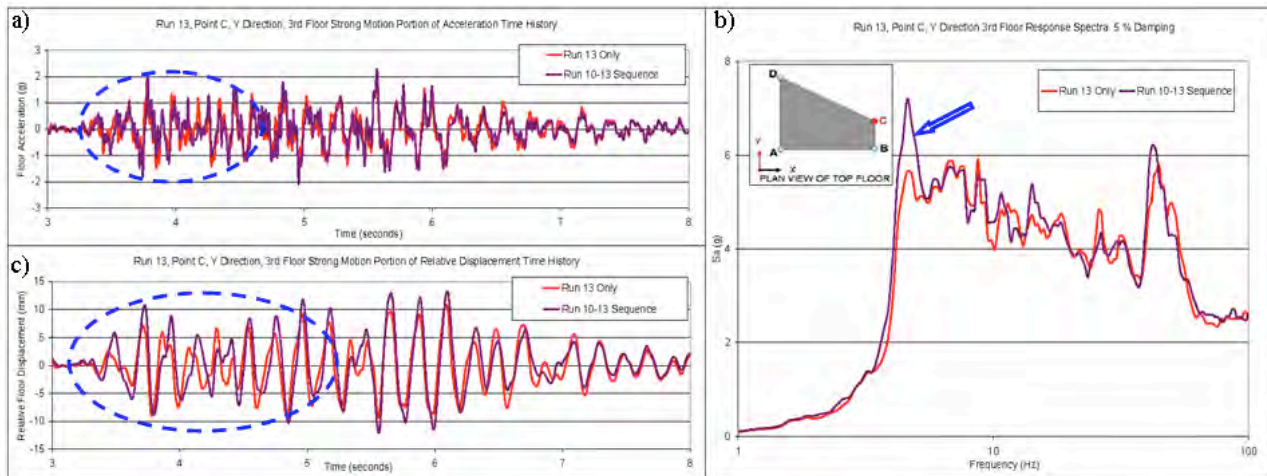


Figure 11. a) Strong motion portion of point C, Y-direction acceleration time histories for run 13. b) Acceleration FRS of point C, Y-direction for run 13. c) Strong motion portion of point C, Y-direction displacement time histories for run 13. (non-linear model results)

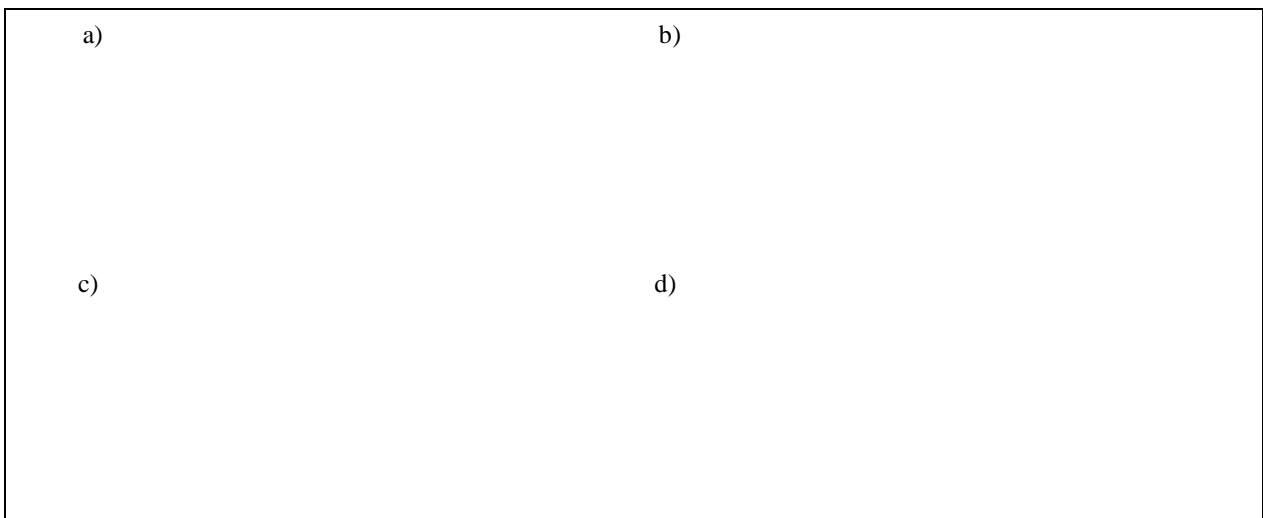


Figure 12. a) Floor peak X-direction horizontal accelerations for run 13. b) Floor peak Y-direction horizontal accelerations for run 13. c) Floor peak X-direction horizontal displacement for run 13. d) Floor peak Y-direction horizontal displacement for run 13. (non-linear model results)

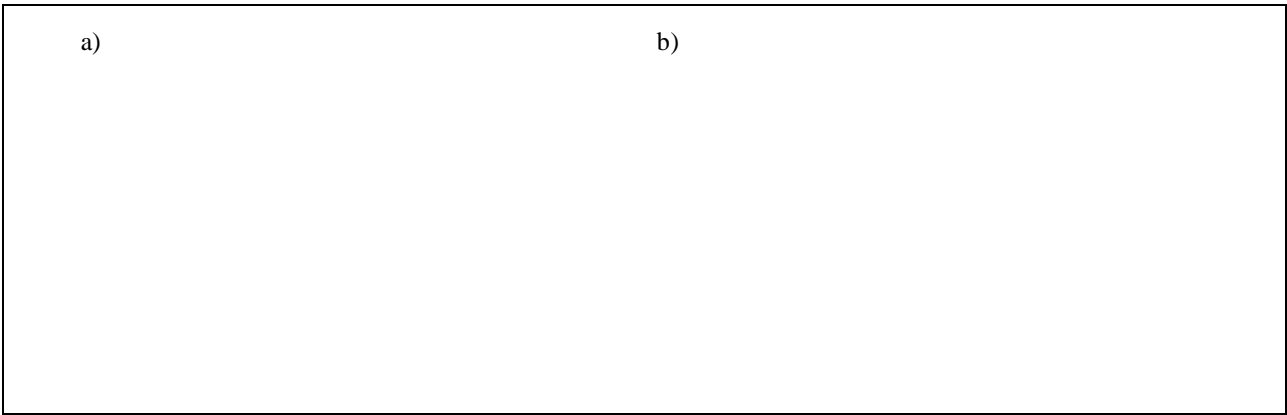


Figure 13. a) Acceleration FRS of point C, X-direction for run 13. b) Acceleration FRS of point C, Y-direction for run 13. (non-linear model results)

6 CONCLUSION

The paper presented the results of various modeling techniques used to predict the seismic performance of the SMART 2008 test specimen. The following conclusions can be drawn from comparison of only the model results:

- The stiffest model, the Linear Design Practice model, predicted the smallest floor accelerations. This indicates that a stiffer model does not necessarily ensure a more conservative result when modeling floor accelerations in a coupled system.
- The Non-Linear Best Estimate model using fiber elements did not consider the improved axial performance of well detailed reinforcement and confined shear wall boundary elements or the influence of reinforcement splices. As a result, we assume that unrealistic stiffness and strength degradation, as well as unrealistic strains were observed in the model response. The improved behavior of the reinforcement splices and the confined shear wall boundary elements is significant to the overall performance of the specimen and should have been considered in the non-linear modeling.
- In many circumstances it is acceptable to ignore the previous events when considering a particular time history event in a sequence of events, as in SMART 2008. Namely, if the specimen remains elastic in the previous events or if the strong motion time history is long enough to give a good representation of the true non-linear condition. However, in the case of run 13 of SMART 2008, the strong motion time history was rather short, and by not considering the initial cracking and non-linearities from the previous runs, the significant portion of the response did not reflect the true non-linear condition.
- The Non-Linear Best Estimate model of the SMART 2008 specimen was relatively insensitive to varying out of plane bending stiffness. This is due to the fact that the model's response is primarily governed by in plane motion as expected from the specimen design.

Acknowledgements. *The authors are grateful to the organizers of the SMART 2008 project, CEA/EDF, for the permission to write this paper and the use of their test specimen as a modeling example. The necessary data was provided by CEA/EDF. Their cooperation is gratefully acknowledged.*

REFERENCES

Lermitte, S., Chaudat, T. 2008. Presentation of the Benchmark Contest-Phase1b-Project SMART 2008. Saclay, France: Commissariat a l'Énergie Atomique (CEA). 33 p. Rapport DM2S, SEMT/EMSI/RT/08-022/A.